23. A. Cassie, S. Baxter, *Trans. Faraday Soc.* **40**, 546–551 (1944).
24. T. Liu, C.-J. Kim, in *Proceedings of the International Conference on Solid State Sensors, Actuators and Microsystems (Transducers'13)*, Barcelona, Spain, 16 to 20 June 2013 (IEEE, Piscataway, NJ, 2013).
25. Y. Ma, X. Cao, X. Feng, Y. Ma, H. Zou, *Polymer (Guildf.)* **48**, 7455–7460 (2007).
26. R. Hensel *et al.*, *Langmuir* **29**, 1100–1112 (2013).
27. This general definitions of f_s and f_g follow Cassie and Baxter's original paper (*23*), which included all of the nonflat (e.g., rough, curved) effects on the liquid-solid and liquid-vapor interface. In addition to the most simplified version of flat liquid-solid and flat liquid-vapor interfaces, which results in $f_s + f_g = 1$, a less simplified version of nonflat liquid-solid and flat liquid-vapor interfaces is often adopted in the literature.
28. Materials and methods are available as supplementary materials on *Science* Online.
29. These liquids are commonly used for applications such as electrochemistry, fuel cells, integrated circuits fabrication, microfluidic systems, heat transfer, etc.

MINERALOGY

Discovery of bridgmanite, the most abundant mineral in Earth, in a shocked meteorite

Oliver Tschauner,[1]* Chi Ma,[2] John R. Beckett,[2] Clemens Prescher,[3] Vitali B. Prakapenka,[3] George R. Rossman[2]

Meteorites exposed to high pressures and temperatures during impact-induced shock often contain minerals whose occurrence and stability normally confine them to the deeper portions of Earth's mantle. One exception has been $MgSiO_3$ in the perovskite structure, which is the most abundant solid phase in Earth. Here we report the discovery of this important phase as a mineral in the Tenham L6 chondrite and approved by the International Mineralogical Association (specimen IMA 2014-017). $MgSiO_3$-perovskite is now called bridgmanite. The associated phase assemblage constrains peak shock conditions to ~ 24 gigapascals and 2300 kelvin. The discovery concludes a half century of efforts to find, identify, and characterize a natural specimen of this important mineral.

In the geosciences, the complexity of compositions and histories of naturally occurring minerals and rocks provides an important ground truth against which experiment and theory are measured. One of the most glaring omissions in the study of Earth's mantle has been the inability to find naturally occurring specimens of what we believe to be Earth's most abundant rock-forming phase, $(Mg,Fe)SiO_3$ in an orthorhombic ABO_3 perovskite structure. Despite appearing for decades in numerous experimental and theoretical studies (*1–5*), characterizations of possible natural samples have not been sufficient to meet International Mineralogical Association criteria for naming a new mineral (*6*). Consequently, any detailed chemical, structural, and petrographic analysis of natural $(Mg,Fe)SiO_3$-perovskite has remained impossible. In addition, having a formal mineral name for a phase that is so important is important in itself. Various ambiguous or incorrect terms such as "silicate perovskite" and "perovskite" have been used for describing this phase, but they convey ambiguity to the description of research findings. We put this ambiguity to rest by describing the natural occurrence of bridgmanite: $MgSiO_3$ in the orthorhombic ABO_3 perovskite structure. The name bridgmanite honors Percy W. Bridgman (1882–1961), the 1946 Nobel laureate in Physics, for his fundamental contributions to high-pressure mineralogy in particular, and to high-pressure research in general.

The importance of bridgmanite in the lower mantle of Earth has long been recognized: Several lines of evidence show that it forms through a

[1]Department of Geoscience and High Pressure Science and Engineering Center, University of Nevada, Las Vegas, NV 89134, USA. [2]Division of Geology and Planetary Science, California Institute of Technology, Pasadena, CA 91125, USA. [3]Center of Advanced Radiation Sources, University of Chicago, Chicago, IL 60632, USA.
*Corresponding author. E-mail: olivert@physics.unlv.edu

Fig. 1. Scanning electron microscope image of a bridgmanite-akimotoite aggregate. The backscatter electron image reveals an aggregate of submicrometer-sized crystals of bridgmanite and akimotoite enclosed in $(Mg,Fe)SiO_3$ glass and within a Tenham shock-melt vein. Majorite is found in the vein matrix. The bridgmanite-akimotoite clast is a pseudomorph after pyroxene that was trapped in the melt. This observation is consistent with an earlier report about the possible occurrence of bridgmanite with akimotoite in Tenham (*16*).
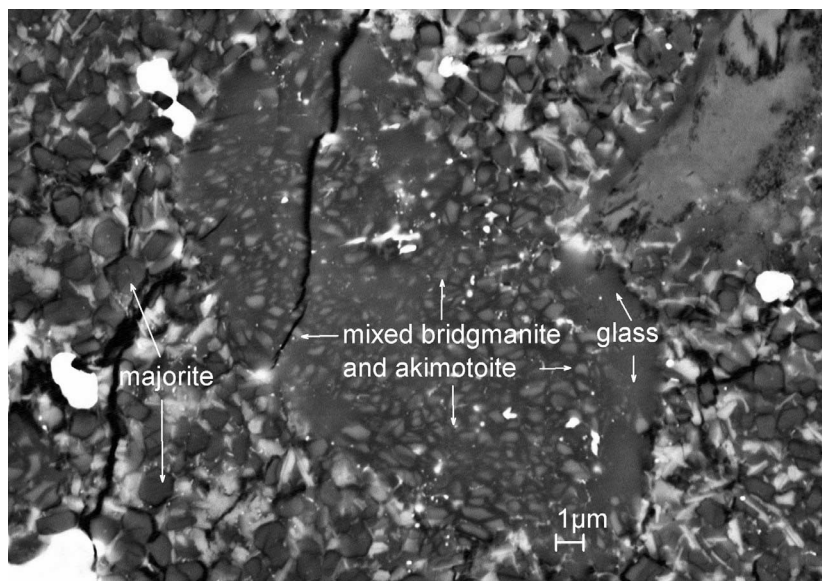
breakdown of rock-forming $(Mg,Fe)_2SiO_4$ into $(Mg,Fe)O$ periclase and $(Mg,Fe)SiO_3$ bridgmanite in the lower mantle of Earth below a depth of 660 km (1–5). Bridgmanite remains stable to the D″ layer, nearly down to the core-mantle boundary region at a depth of 2900 km (7). Thus, bridgmanite makes up about 38 volume % of the entire Earth (4). The chemical and physical properties of bridgmanite have a large influence on elemental distribution, mass flow, and heat flow within Earth's mantle. Numerous efforts have all failed to find a naturally occurring example of this elusive mineral for several reasons. Most im-

portantly, $(Mg,Fe)SiO_3$ in the perovskite structure is stable only at very high pressures and temperatures (8). The mineral is metastable under ambient conditions but vitrifies above temperatures as low as 310 K (9). The exhumation of rocks originating in the lower mantle is far too slow to permit the preservation of terrestrial bridgmanite, although inclusions in some diamonds from such rocks have been interpreted as the breakdown products of bridgmanite (10, 11). Heavily shocked meteorites provide an alternative route for preserving bridgmanite. Pressures and temperatures during the shock event can be high

enough to stabilize bridgmanite, and the release to ambient conditions may be sufficiently fast to kinetically inhibit breakdown reactions. As a result, several high-pressure phases known to be stable only deep within Earth's mantle have been found as minerals in these meteorites (12–18). These observations instigated decades of efforts to find and characterize bridgmanite in shocked meteorites (15–19). Meticulous transmission electron microscopy examination yielded indications of the presence of bridgmanite in chondritic and martian meteorites (15–19). However, rapid vitrification in the electron beam, a lack of adequate sets of reflections for unique crystallographic indexing, and the absence of quantitative structure factor moduli rendered these observations insufficient to characterize a new mineral.

A different approach to the search for bridgmanite lies in using microfocused high-energy synchrotron x-ray beams instead of electron beams for diffraction. The intense high-energy x-ray beam does little to damage bridgmanite because of its low absorbance. Micro-focusing and novel fast readout area detector techniques permit efficient mapping of possible host regions in shocked meteorites (20). Our search focused on shock-melt veins and their inclusions, which were previously identified as the hosts of other high-pressure silicate phases (12–20). In particular, we examined the highly shocked Tenham L6 chondrite and identified bridgmanite in clasts within the shock-melt veins. We found bridgmanite always associated with akimotoite but never as isolated crystals in the melt vein. These two phases along with a vitreous matrix whose composition is identical within error to that of the bridgmanite (table S1) replace precursor orthopyroxene crystals trapped within a melt vein (Fig. 1 and fig. S1). We interpret this assemblage to reflect bridgmanite that partially vitrified upon release from the shock state on the parent body or during its residence on Earth after its fall in 1879. We hypothesize that the volume expansion upon transformation from bridgmanite or dense glass into normal glass by ~ 33% (21) and 1 to 2% (22), respectively, induces stresses in the surrounding rock that help preserve the remaining bridgmanite.

Bridgmanite assumes the Pnma perovskite structure with unit cell parameters $a = 5.02 \pm 0.03$ Å, $b = 6.90 \pm 0.03$ Å, and $c = 4.81 \pm 0.02$ Å, which yield a unit cell volume of 167 ± 2 Å^3 (Fig. 2) (23). The uncertainties (± SEM) are from (i) uncertainty in the Rietveld refinement (see Fig. 2) and (ii) variations in cell parameters due to varying chemical composition (fig. S2). Akimotoite and ringwoodite also contribute to the diffraction pattern. The average composition of the type material (table S1) has a formula unit of $(Mg_{0.75}Fe_{0.20}Na_{0.03}Ca_{0.02}Mn_{0.01})Si_{1.00}O_3$ (23). The composition is well within the range of synthetic bridgmanites, despite being a quite sodic and Fe-rich composition in comparison (fig. S2).

The cell volume of natural bridgmanite lies on an extension of the trend of volume expansion along with increasing Fe^{3+} content (24), which is consistent with a large amount of ferric iron as

Fig. 2. Powder diffraction pattern and Rietveld refinement of bridgmanite. The figure shows the observed diffraction pattern (black line and symbols) of bridgmanite-bearing shock-melt vein material in thin section USNM 7703 (23), whole pattern refinement (red), refined pattern of bridgmannite (blue), residual of fit (green), and positions of observed reflections of bridgmanite, akimotoite, and ringwoodite (blue, red, and green tick marks, respectively). The x-ray wavelength was 0.3344 Å. The weighted-profile refinement factor was

0.08, and there were 799 observations. The examined portion of the Tenham meteorite revealed diffraction by bridgmanite, akimotoite, and ringwoodite in relative volume proportions of 11, 16, and 74%. Ringwoodite forms clasts within the shock-melt vein (fig. S1), some of which occur beneath the examined akimotoite-bridgmanite-glass clast (the x-ray beam covers a 3 × 4 μm² area but it passes through the entire ~30–μm-thick rock section). The bridgmanite-akimotoite aggregate has a volume proportion ~ 0.7:1, in accord with scanning electron microscope examination. rel., relative; a.u., arbitrary units.
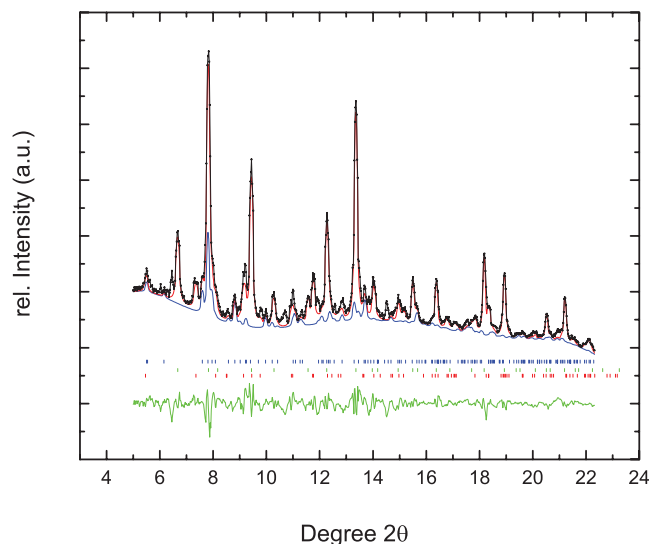
Fig. 3. Correlation of unit cell volume with Fe content in synthetic and natural bridgmanite. Bridgmanites with dominantly ferrous iron exhibit a weak increase in volume with increasing iron content [dashed curve (24)]. Bridgmanites with large concentrations of ferric iron (24, 63) exhibit a more pronounced increase of volume with increasing Fe content (squares). Natural bridgmanite ranges in cell volumes due to chemical variations (fig. S2) as

indicated by the hached region. However, the average volume of natural bridgmanite from Tenham lies on an extension of the trend established by synthetic ferric bridgmanite. The black vertical bar indicates an approximate uncertainty for the volume measurements on synthetic bridgmanite based on the single-crystal diffraction studies of the Mg end member at ambient pressure (63–66). pfu, per formula unit.
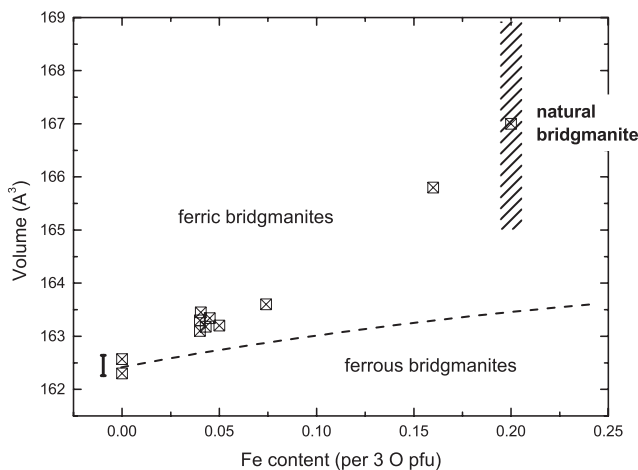
compared to synthetic bridgmanites (Fig. 3). As noted above, the holotype specimen of bridgmanite also contains high concentrations of Na. This may extend the stability field of bridgmanite (25) and supports charge balance for ferric iron via Na-Fe^{3+}–coupled substitution in holotype bridgmanites at redox conditions below the iron-wüstite buffer (26), but plausibly also in the terrestrial and martian (27) lower mantles.

The evaluation of the shock conditions in Tenham beyond the examination of plausible recovery paths for bridgmanite is outside the scope of this study. The strict association of akimotoite and bridgmanite and the likely absence of bridgmanite in the matrix of the shock-melt vein are pivotal to an assessment (fig. S3). They suggest that the peak pressure exceeded 23 GPa, with temperatures in the melt exceeding the solidus at ~2200 K. The absence of bridgmanite as isolated crystals within the shock-melt vein suggests that pressures were too low to permit crystallization from melt. Using these constraints, we estimate the conditions of formation of bridgmanite in Tenham to be 23 to 25 GPa and 2200 to 2400 K (fig. S3). This estimate is consistent with a more recent estimate by Xie et al. (20) based on observation of vitrified bridgmanite. The occurrence of bridgmanite along with conditions of formation of other high-pressure minerals imposes strong constraints on pressure and temperature conditions during high-level shock events in meteorites.

REFERENCES AND NOTES

1. L. Liu, Geophys. Res. Lett. 1, 277–280 (1974).
2. A. E. Ringwood, Geochim. Cosmochim. Acta 55, 2083–2110 (1991).
3. R. J. Hemley, R. E. Cohen, Annu. Rev. Earth Planet. Sci. 20, 553–600 (1992).
4. L. Stixrude, C. Lithgow-Bertelloni, Annu. Rev. Earth Planet. Sci. 40, 569–595 (2012).
5. E. Ito, E. Takahashi, Y. Matsui, Earth Planet. Sci. Lett. 67, 238–248 (1984).
6. E. H. Nickel, J. D. Grice, Can. Mineral. 36, 913–926 (1998).
7. M. Murakami, K. Hirose, N. Sata, Y. Ohishi, Geophys. Res. Lett. 32, L03304 (2005).
8. L. Stixrude, C. Lithgow-Bertelloni, Geophys. J. Int. 184, 1180–1213 (2011).
9. D. J. Durben, G. H. Wolf, Am. Mineral. 77, 890–893 (1992).
10. S. E. Kesson, J. D. Fitz Gerald, Earth Planet. Sci. Lett. 111, 229–240 (1992).
11. F. E. Brenker, T. Stachel, J. W. Harris, Earth Planet. Sci. Lett. 198, 1–9 (2002).
12. R. A. Binns, R. J. Davis, S. J. B. Reed, Nature 221, 943–944 (1969).
13. J. V. Smith, B. Mason, Science 168, 832–833 (1970).
14. G. D. Price, A. Putnis, S. O. Agrell, D. G. W. Smith, Can. Min. 21, 29–35 (1983).
15. N. Tomioka, K. Fujino, Am. Mineral. 84, 267–271 (1999).
16. T. G. Sharp, C. M. Lingemann, C. Dupas, D. Stöffler, Science 277, 352–355 (1997).
17. H. Mori, J. Mineral. Soc. Japan 23, 171–178 (1994).
18. N. Miyajima et al., Am. Mineral. 92, 1545–1549 (2007).
19. M. Miyahara et al., Proc. Natl. Acad. Sci. U.S.A. 108, 5999–6003 (2011).
20. D. Z. Xie, T. G. Sharp, P. S. DeCarli, Geochim. Cosmochim. Acta 70, 504–515 (2006).
21. S.-N. Luo, J. A. Akins, T. J. Ahrens, P. D. Asimow, J. Geophys. Res. 109 (B5), B05205 (2004).
22. C. Sanchez-Valle, J. D. Bass, Earth Planet. Sci. Lett. 295, 523–530 (2010).
23. See the supplementary materials.
24. D. R. Hummer, Y. W. Fei, Am. Mineral. 97, 1915–1921 (2012).
25. B. Grocholski, K. Catalli, S.-H. Shim, V. Prakapenka, Proc. Natl. Acad. Sci. U.S.A. 109, 2275–2279 (2012).
26. H. Y. McSween Jr., T. C. Labotka, Geochim. Cosmochim. Acta 57, 1105–1114 (1993).
27. C. M. Bertka, Y. Fei, J. Geophys. Res. 102, 5251–5264 (1997).

CHEMICAL OCEANOGRAPHY

Increasing anthropogenic nitrogen in the North Pacific Ocean

Il-Nam Kim,[1] Kitack Lee,[1]* Nicolas Gruber,[2] David M. Karl,[3] John L. Bullister,[4] Simon Yang,[2] Tae-Wook Kim[5]

The recent increase in anthropogenic emissions of reactive nitrogen from northeastern Asia and the subsequent enhanced deposition over the extensive regions of the North Pacific Ocean (NPO) have led to a detectable increase in the nitrate (N) concentration of the upper ocean. The rate of increase of excess N relative to phosphate (P) was found to be highest (~0.24 micromoles per kilogram per year) in the vicinity of the Asian source continent, with rates decreasing eastward across the NPO, consistent with the magnitude and distribution of atmospheric nitrogen deposition. This anthropogenically driven increase in the N content of the upper NPO may enhance primary production in this N-limited region, potentially leading to a long-term change of the NPO from being N-limited to P-limited.

The rate of deposition of reactive nitrogen (i.e., $NO_y + NH_x$ and dissolved organic forms; see supplementary text S1) from the atmosphere to the open ocean has more than doubled globally over the past 100 years (1), reaching a magnitude that is comparable to about half of the global ocean N_2 fixation (2). The increase in atmospheric nitrogen deposition (AND) is particularly acute in the North Pacific Ocean (NPO) due to rapid population growth and burgeoning industrial activity in northeast Asian countries. These changes in northeast Asia have markedly increased reactive nitrogen fluxes in the adjacent marine environment (3, 4), largely through atmospheric transport by westerly winds and subsequent deposition. Though it has been recognized that such an increasing addition of reactive nitrogen to the ocean could lead to major changes in the upper ocean nitrogen cycle and biological productivity (5), the majority of studies conducted to date have suggested that the impact is small and not detectable (1), except in near-shore environments and marginal seas (3). A recent study directly comparing nutrient measurements made over more than two decades showed that nitrate (N) concentration has increased in the northeast Asian marginal seas and that this increase was probably due to strongly growing AND (3). Here we extend this analysis to the entire NPO and show that the anthropogenic influence has already affected the open-ocean nitrogen cycle.

Owing to a lack of basin-wide, nutrient concentration data of sufficient duration (decades) at strategic locations, we reconstructed the temporal changes in N across the NPO using a method based on the relation between the excess of N in a water parcel relative to that expected based on the phosphate (P) concentration and the chlorofluorocarbon-12 (CFC-12)–derived ventilation age of that water parcel (6) (supplementary text S2). The excess in N relative to P—i.e., N^* (7, 8)—at each sampling location was calculated as: $N^* = N - R_{N:P} \times P$, where N and P are the measured concentrations and $R_{N:P}$ is the Redfield ratio of 16:1. Because of increasing

[1]School of Environmental Sciences and Engineering, Pohang University of Science and Technology (POSTECH), Pohang, 790–784, Republic of Korea. [2]Environmental Physics Group, Institute of Biogeochemistry and Pollutant Dynamics, ETH Zürich, Zürich, Switzerland. [3]Daniel K. Inouye Center for Microbial Oceanography, University of Hawaii at Manoa, 1950 East West Road, Honolulu, HI 96822, USA. [4]Pacific Marine Environmental Laboratory, National Oceanic and Atmospheric Administration (NOAA), Seattle, WA 98115, USA. [5]Ocean Circulation and Climate Research Division, Korea Institute of Ocean Science and Technology, Ansan, 426–744, Republic of Korea.

*Corresponding author. E-mail: ktl@postech.ac.kr